Journal of Thermal Engineering, Vol. 4, No. 2, Special Issue 7, pp. 1791-1802, February, 2018
Yildiz Technical University Press, Istanbul, Turkey

USING OF FLOW ROUTING PLATE FOR COOLING OF PRINTED CIRCUIT BOARDS

B. Kurşun[1,*], M. Sivrioğlu[2]

ABSTRACT

Effective cooling of electronic components plays an important role in system design and efficiency. In this study, the effects of using the flow routing plate in cooling printed circuit boards have been investigated. For this purpose, effects of the flow routing plate on the laminar mixed convection heat transfer from protruded heat sources at the side walls of the horizontal channel, were investigated numerically. The air was used as cooling fluid, and protruded heat sources were equipped as rows into the rectangular channel with insulated walls. Numerical investigations were carried out for different plate inclination angles at different Reynolds and modified Grashof numbers. It is observed that the using of flow routing plate increases the heat transfer at different ratios by comparison to the case without plate and enhances the cooling conditions for all values of parameters in the analyses. The highest heat transfer enhancement occurred at values where Reynolds number (Re) was Re = 1000 and plate inclination angle (α) was α = 60 °.The results obtained during the numerical analyses are presented in detail in the form of graphics for the row averaged Nusselt number, heater temperatures, velocity vectors, and temperature contours.

Keywords: *Horizontal channel, Flow routing plate, Mixed convection, Protruded heat sources*

INTRODUCTION

Reducing the size of electronic devices and increasing the number of circuits increases the heat generation in the electronic chips and can cause damage over a certain temperature value. In the literature studies, many cooling methods have been developed for the purpose of preventing the temperature increases which cause damage. In these studies, chips in electronic circuit boards were modeled as rectangular heat sources. In the Wu and Pergn's numerical study, mixed convection heat transfer from protruding heat sources placed at the bottom of the channel was investigated at the different Re and Gr numbers for the use of a plate placed at the angle to the channel entrance [1]. Numerical results showed that the maximum heat transfer increase with plate placement occured for the plate inclination angle of 30º. Korichi et al. investigated the effect of the periodic plate placement on the heat transfer from the heaters in a horizontal channel for variable parameters as plate lengths, angles and Reynolds numbers [2]. With the plate placement on the upper surface of the channel, the heat transfer is increased by creating vortex flow of different sizes. It has been observed that heat transfer is further increased according to the use of grooved channels. Davidson, however, conducted the effect of inclination angle and thickness of a plate that placed in a channel, on heat transfer and pressure drop. [3] In the study, it was demonstrated that plate placement increases heat transfer and pressure loss. Also the effects of numerical solution methods on results were investigated. In a numerical study carried out by Sohankar, the effects of the V-shaped plate placement in a rectangular horizontal channel on the heat transfer and pressure drop depending on the inclination angle of the plate and channel height were investigated [4]. Numerical results showed that the increase in the Re number and plate inclination angle provides an increase in heat transfer. It is also investigated DNS and LES solution procedure and compared with eachother. Beig has carried out a numerical study in order to determining the most suitable position of a flow routing plate in the channel and revealed that the optimum position of the plate was independent from Re number [5]. It has been found that the best position of the plate is at the channel entrance in terms of heat transfer enhancement and flow uniformity. Abdollahi and Shams implemented a numerical study to find the optimal plate shape and slope angle by using the Pareto optimization strategy [6]. It was found that the effect of plate angle on the heat transfer was low in low Re number values, but increased heat transfer and pressure drop in high Re number values. In another study carried out by Calışkan, it was aimed to increase the heat transfer by using a punched triangular and rectangular vortex generators in the channel flow [7]. The best heat transfer enhancement about 23-55% was obtained with the punched triangular vortex generator for different winglet attack

This paper was recommended for publication in revised form by Regional Editor Omid Mahian
[1]Department of Mechanical Engineering, Amasya University, Amasya, TURKEY
[2]Department of Mechanical Engineering, Gazi University, Ankara, TURKEY
**E-mail address: burak.kursun@amasya.edu.tr*
Manuscript Received 24 February 2017, Accepted 22 April 2017

angles. Zhou and Feng investigated the effect of the plane and curved winglet (rectangular, trapezoidal and delta) vortex generators with and without punched holes on the heat transfer in the channel flow [8]. The results showed that the best heat transfer enhancement was achieved by using of curved winglet vortex generator. In the experimental study performed by Chen et al., however, the effect of various longitudinal vortex generators on heat transfer was investigated in a rectangular microchannel for different aspect ratio of the channel [9]. Results obtained from the experimental study indicated that the highest increase in heat transfer and pressure drop occurred for low value of aspect ratio. It has been reported that the use of flow routing objects has also increased heat transfer in other studies carried out except the channel flow [10-15].The studies available in the literature show that the placement of flow routing objects (plate, cylinder etc.) in the channel affects the heat transfer rate at different ratios depending on the parameters such as the layout of the heat sources, plate angle, plate length and thickness, Re number, and aspect ratio.

In the studies related to the investigation of the effect of placing flow routing objects inside the channel on heat transfer from the heaters, the heaters are placed only on the channel bottom or top surface. There is no detailed study of the use of flow routing plates when heat sources are placed on the channel side surfaces. In this study, however, the effects of the use of the flow routing plate on the heat transfer from the heaters are investigated numerically by forming a model in which the heat sources are located on the side surfaces of the channel. In internal channel flow conditions, where heat sources are placed vertically, was provided 30-55% heat transfer increase with the use of flow rotuing plate.

PHYSICAL MODEL

The problem addressed in this study is the effect of the use of the flow routing plate on the heat transfer from protruding heat sources in a horizontal channel. The geometries formed in the case with and without plate are given in Figure 1. As can be seen in Figure. 1, the protruding heat sources are located on the channel side surfaces and the flow routing plates are located between the first heater rows.

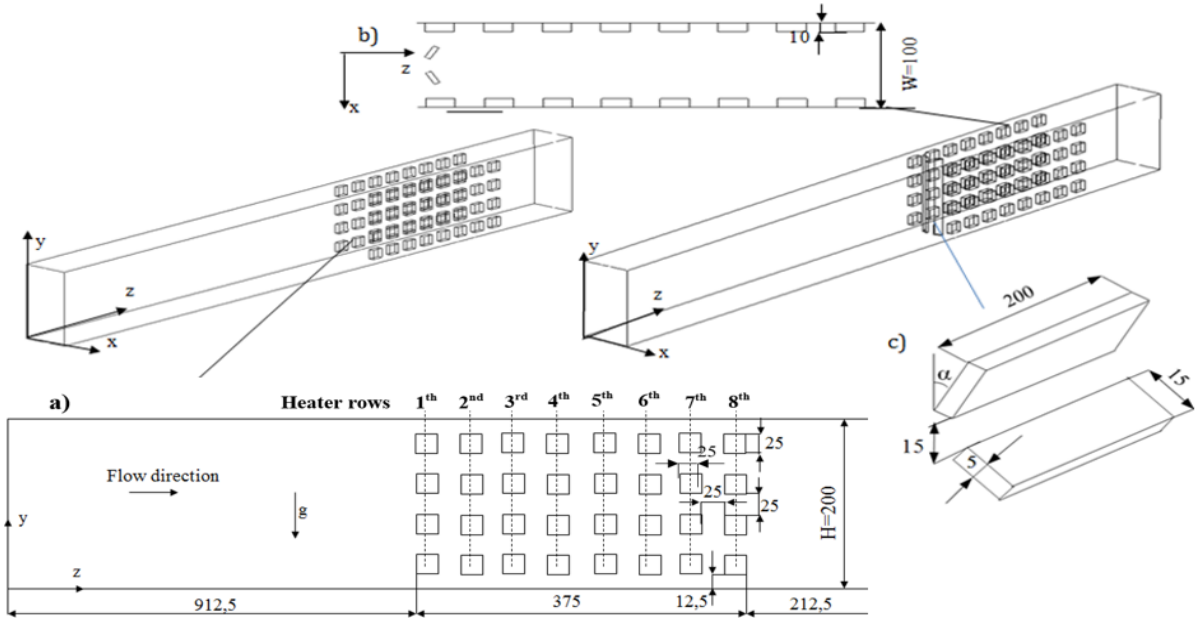

Figure 1. Channel geometry (dimensions in mm.) a) Dimension of channel and heater zone, b) Layout of plates

MATHEMATICAL MODEL

In the study, air was used as a coolant and analyzes were made assuming that the fluid was newtonian, incompressible, and the physical properties were constant under laminar flow conditions. In addition, the Boussinesq approach is used to determine the effect of buoyant force. The conservation equations used to find the velocity components (u, v, w), pressure (P) and temperature (T) of the flow in the study are given below.

Conservation of mass for three-dimensional cartesian co-ordinates under laminar flow conditions can be written as shown by Eq. (1).

$$\frac{\partial(\rho u)}{\partial x}+\frac{\partial(\rho v)}{\partial y}+\frac{\partial(\rho \mathrm{w})}{\partial z}=0 \tag{1}$$

Equation (2), (3) and (4) denote the conservation equations of momentum in x, y and z directions respectively,

$$\mathrm{u}\frac{\partial(\rho u)}{\partial x}+v\frac{\partial(\rho u)}{\partial y}+w\frac{\partial(\rho u)}{\partial z}=-\frac{\partial P}{\partial x}+\mu(\frac{\partial^2 u}{\partial x^2}+\frac{\partial^2 u}{\partial y^2}+\frac{\partial^2 u}{\partial z^2}) \tag{2}$$

$$u\frac{\partial(\rho v)}{\partial x}+v\frac{\partial(\rho v)}{\partial y}+w\frac{\partial(\rho v)}{\partial z}=-\frac{\partial P}{\partial y}+\mu(\frac{\partial^2 v}{\partial x^2}+\frac{\partial^2 v}{\partial y^2}+\frac{\partial^2 v}{\partial z^2})+\rho g\beta(T-T_{inlet}) \tag{3}$$

$$u\frac{\partial(\rho w)}{\partial x}+v\frac{\partial(\rho w)}{\partial y}+w\frac{\partial(\rho w)}{\partial \mathrm{z}}=-\frac{\partial P}{\partial z}+\mu(\frac{\partial^2 w}{\partial x^2}+\frac{\partial^2 w}{\partial y^2}+\frac{\partial^2 w}{\partial z^2}) \tag{4}$$

In the differential equations given above, u, v and w are the velocity components in the x, y and z directions respectively, P is fluid pressure, μ is the dynamic viscosity of the fluid, ρ is the fluid density, g is the acceleration of gravity, β is the coefficient of thermal expansion at the channel inlet temperature, T is the fluid temperature, T_{inlet} is the inlet temperature of the fluid. In Eq. (3), the last expression on the right side of the equation is used to determine the effect of the mass forces (Boussinesq approach).

The conservation of the energy is given by Eq. (5),

$$\mathrm{u}\frac{\partial(\rho T)}{\partial x}+v\frac{\partial(\rho T)}{\partial y}+w\frac{\partial(\rho T)}{\partial z}=\frac{k}{c_P}(\frac{\partial^2 T}{\partial x^2}+\frac{\partial^2 T}{\partial y^2}+\frac{\partial^2 T}{\partial z^2}) \tag{5}$$

Where c_p is the specific heat of the fluid and k is the thermal conductivity coefficient of the fluid.

The boundary conditions for the channel inlet and outlet used in the solution of the differential equations are given in Eqs. (6) and (7), respectively,

$$\mathrm{u}=0, v=0, w=wgiriş, T=T_{inlet}, P=P_{atm} \tag{6}$$

$$\frac{\partial u}{\partial z}=0,\frac{\partial v}{\partial z}=0,\frac{\partial w}{\partial z}=0,\frac{\partial T}{\partial z}=0 \tag{7}$$

The flow in the channel is symmetric with respect to the plane x = W / 2 passing through the channel center. The corresponding symmetry boundary conditions are given by Eq. (8),

$$\mathrm{u}=0,\frac{\partial v}{\partial x}=0,\frac{\partial w}{\partial x}=0,\frac{\partial T}{\partial x}=0,\frac{\partial P}{\partial x}=0 \tag{8}$$

On the bottom, top and side surfaces of the channel and on the surfaces of plates and heat sources, no-slip conditions are defined and these surfaces are assumed to be insulated so that the heat flux on the surfaces is zero except the surface of heaters (Eq. 9).

$$u=0, v=0, w=0, \dot{q}=0 \tag{9}$$

The boundary condition on the heater surfaces is as given in Eq. (10),

$$\dot{q} = \dot{q}_{conv.} \tag{10}$$

NUMERICAL METHOD

The finite volume method was used to solve the problem and numerical analyzes were performed using the ANSYS Fluent software. Because of the symmetry in the model of the flow in the channel, half of the channel geometry given in Figure. 1 is modeled. The boundary conditions above mentioned used to solve the conservation equations were defined as "velocity inlet" at channel inlet, "outflow" at channel outlet and "wall" at solid surfaces in CFD program. In addition, constant heat flux values are assigned to each heater surface as described in Eq. (10).

SIMPLE algorithm is used for discretization and solution of conservation equations in the case without plate. In the case with plate, however, Coupled algorithm with Pseudo Transient option is used because it facilitates convergence in the flow conditions in which natural convection predominates [16].The standard method for the pressure correction and the Second Order UPWIND scheme for the momentum and energy equations were chosen to find the intermediate point values in the algebraic equations obtained as a result of the discretization process. The analyzes continued until the residual values were 1x10-6 for mass and momentum conservation, and 1x10-10 for energy equations.

ANALYZING OF NUMERICAL DATA

Numerical analysis was performed by giving constant and uniform heat flux values to each heater and dimensionless parameters affecting heat transfer were calculated by using the following equations.
The Reynolds number (Re) was found by Eq. (11),

$$\mathrm{Re} = \frac{w_{inlet} D_H}{v} \tag{11}$$

Where w_{inlet} is the velocity of air at the channel inlet and ν is the kinematic viscosity of the air. Hydraulic diameter (D_H) is calculated as follows,

$$D_H = \frac{4A_k}{P_ç} \tag{12}$$

In this equation, A_k is the cross-sectional area of the channel, P_c is the perimeter of the channel.
Eq. (13) was used to calculate the Grashof number (Gr),

$$\mathrm{Gr} = \frac{g\beta(T_s - T_{inlet})_{ave.} D_H^3}{v^2} \tag{13}$$

Where T_s is the heater surface temperature, T_{inlet} is the inlet air temperature, and $(T_s\text{-}T_{inlet})_{ave.}$ value is the average temperature difference of 64 heaters.

The modified Grashof number (Gr *) is expressed by the following equation,

$$\mathrm{Gr}^* = \frac{g\beta\dot{q}_{conv.ave.} D_H^4}{kv^2} \tag{14}$$

Where $q_{conv.ave.}$ is the average convection heat flux in 64 heaters and k is the thermal conductivity of air.
The row average Nusselt number ($Nu_{row\ ave.}$) is calculated by the following equation,

$$Nu_{row\ ave.} = \frac{hD_H}{k} \tag{15}$$

Where h denotes the convective coefficient of air and is found by Eq. (16),

$$h = \frac{\dot{q}_{conv.\ row\ ave.}}{(T_s - T_{inet})_{row\ ave.}} \tag{16}$$

In Eq. (16), $\dot{q}_{conv.\ row\ ave.}$ represents the average convection heat flux for the heater rows consisting of four heater blocks, and $(T_s - T_{inlet})_{row\ ave.}$ represents the average row temperature difference. If Eq. (16) is substituted in Eq. (15), the following expression is obtained for $Nu_{row\ ave.}$,

$$Nu_{row\ ave.} = \frac{\dot{q}_{conv.\ row\ ave.} D_H}{k(T_s - T_{inlet})_{row\ ave.}} \tag{17}$$

In order to understand the effect of the flow regime on the heat transfer, the Richardson number (Ri) is calculated by Eq. (18). Mixed convection condition is assumed when Ri number is approximately Ri = 1, the condition in which natural convection predominates is assumed for Ri>>1, and the condition in which forced convection predominates is assumed for Ri<<1 (18).

$$\mathrm{Ri} = \frac{\mathrm{Gr}}{Re^2} \tag{18}$$

VERIFICATION OF NUMERICAL RESULTS

Numerical results are compared with the results of the experimental study conducted by Kurşun [17] to validation. In the experimental study conducted by Kurşun, the heaters were placed on the upper and lower surface of a horizontal rectangular channel, and the flow routing plates were placed in the inlet of the heater zone (Figure 2). Starting from the rough mesh structure on the model considered for comparison, various mesh structures were formed and the most suitable mesh structure which is compatible with the experimental results was obtained. Mesh structures with 64x80x377 points and 80x80x430 points along the x, y, and z axes, respectively, for the cases with and without plate, comply with the experimental results. For most of the computational domain, an uniform mesh structure was used and the number of cells towards the heater, plate and channel surfaces was increased. The mesh structure and cell distribution generated for the verification of numerical solutions are shown in Figure 2. The graphs in Figure 3 show the comparison of the Nu number values according to the heater row number with the experimental results for a certain Re number in the cases with and without plate. In Figure 3., it is seen that the maximum error is 7%, compared to that of experimental study results. This indicates that the solution method and numerical model are in good agreement with the experimental results.

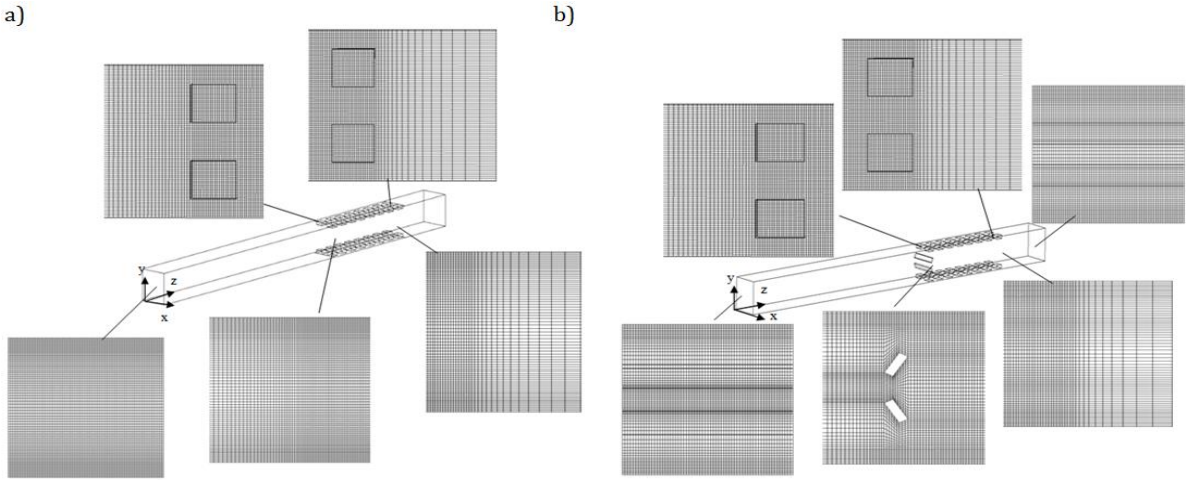

Figure 2. Mesh structure and cell distrubution for validation [17] a) without plate b) with plate (α=30˚)

In this study, the identical mesh structure and cell distribution as in Figure 2 are used. Unlike the geometry in Figure 2, only the heaters are placed in the channel side surfaces (Figure 4). In other words, the heater rows are

rotated in the direction of the y-axis, and the numerical solution is performed for half the channel geometry due to the symmetry on the plane passing through the center of the x-axis.

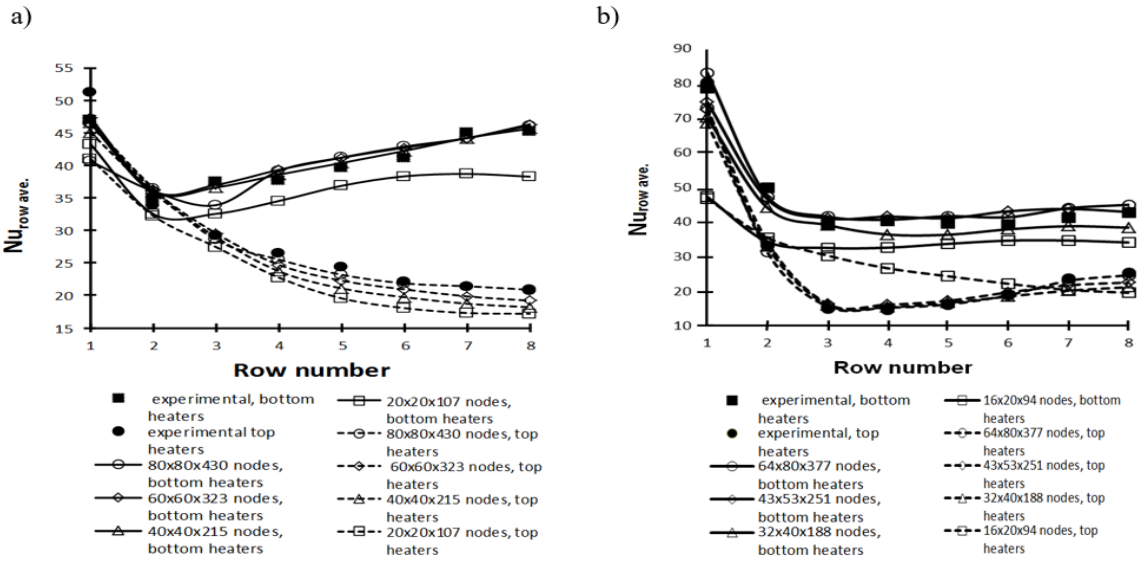

Figure 3. Grid independent test and comparison with experimental results for different numbers of node (Re=2000, Gr*=3x10^8, α=30˚) a) without plate b) with plate

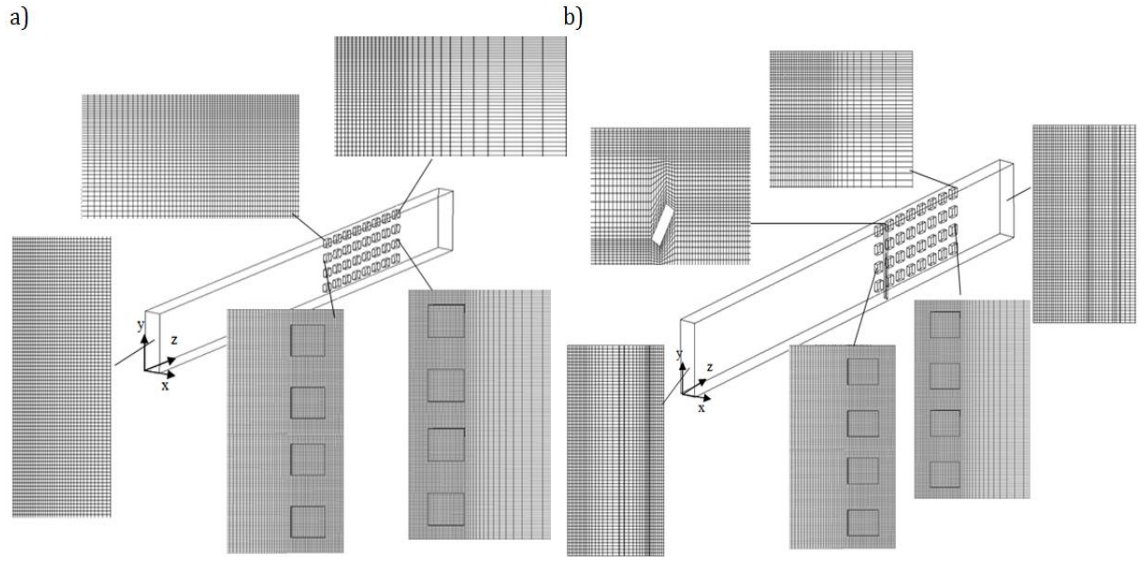

Figure 4. Mesh structure and cell distribution for the present study a) without plate b) with plate (α=30˚)

RESULTS AND DISCUSSION

The numerical study was carried out for variable Reynolds (Re) and modified Grashof (Gr *) numbers at 0 °, 30 °, 60 ° inclination angles (α) of the flow routing plates (Table 1).

Table 1. Numerical study parameters

All cases		Case without plate	Case with plate	
Re	**Gr***	**Ri**	**α**	**Ri**
1000	1.5x10^8	5.6	30°	5
1000	1x10^8	2.4	30°	3.4
1000	5x10^7	2.1	30°	1.8
860	1.5x10^8	8.2	30°	7.4
600	1.5x10^8	20	30°	19
1000	1.5x10^8	5.6	60°	4.5
1000	1.5x10^8	4	0°	5.1

As can be seen in Figure 5a, for all values of Gr *, the heater temperatures are reduced by using of plate at the inlet of the heater zone when the cases with and without plate are compared with each other. It can be seen that the first heater rows are affected most by the change of Gr * number. When all the heater rows are considered, it is understood that the increase of heat transfer according to the case without plate at Gr * = 1x108 is the highest. For the other Gr * values, the increase in heat transfer decreases according to the case without plate. This indicates that the increase in the number of Gr * as well as the increase in the natural convection effect contributes positively to the increase in heat transfer up to a certain value of Ri. The values of Ri number ranged from 1.8 to 20, as shown in Table 1.

Another important factor affecting the amount of heat transfer is the change in the Re number. In the graphs given in Figure 5b, it is seen that the value of Nurow ave. number in the first heater row greatly increases in all values of Re by the effect of plate placement on the heater zone entrance. In other heater rows, the amount of heat transfer decreases with the decrease of air velocity. It is seen that the increase of the heat transfer according to the case without plate reaches its maximum value at Re = 1000. The forced convection effect is negligible (Ri = 19) and a flow of natural convection conditions occurs for the value of Re = 600. In this case, there is a significant heat transfer increase only for the first heater row by using of plate.

Figure 5c shows that when the plate angle is α = 30 ° and α = 0 °, the Nurow ave. number takes approximately the same values except for the first two heater row and in both cases, more efficient cooling conditions have been achieved by increasing the amount of heat transfer according to the case without plate. For α = 60 °, it is seen that the heat transfer from the all heater row is higher than the heat transfer at other angle values.

In Figures (6)-(9), the velocity vectors and the temperature contours are given in the cases with and without plate according to the Gr * number change. When the y-z plane velocity vectors in the case with plate for Gr * = 1.5x108 were examined (Figure 6a), the increase in the heat transfer with the increase of the air velocity at the position of the first heater row become the greatest. After the second heater row, the air velocity decreases and the air flow directs toward the upper surface of the channel with the effect of natural convection. This situation, as shown in Figure 6c, causes the temperatures in the heaters near the top surface to increase. Furthermore, the air that passes between the plate and the heater strikes the heater surface, which first diverts toward the center of the channel and then leaves the channel in parallel with the heater surfaces (Figure 6b). This situation has led to insufficient air flow and increased temperatures in the heaters of the 2-4. heater rows.

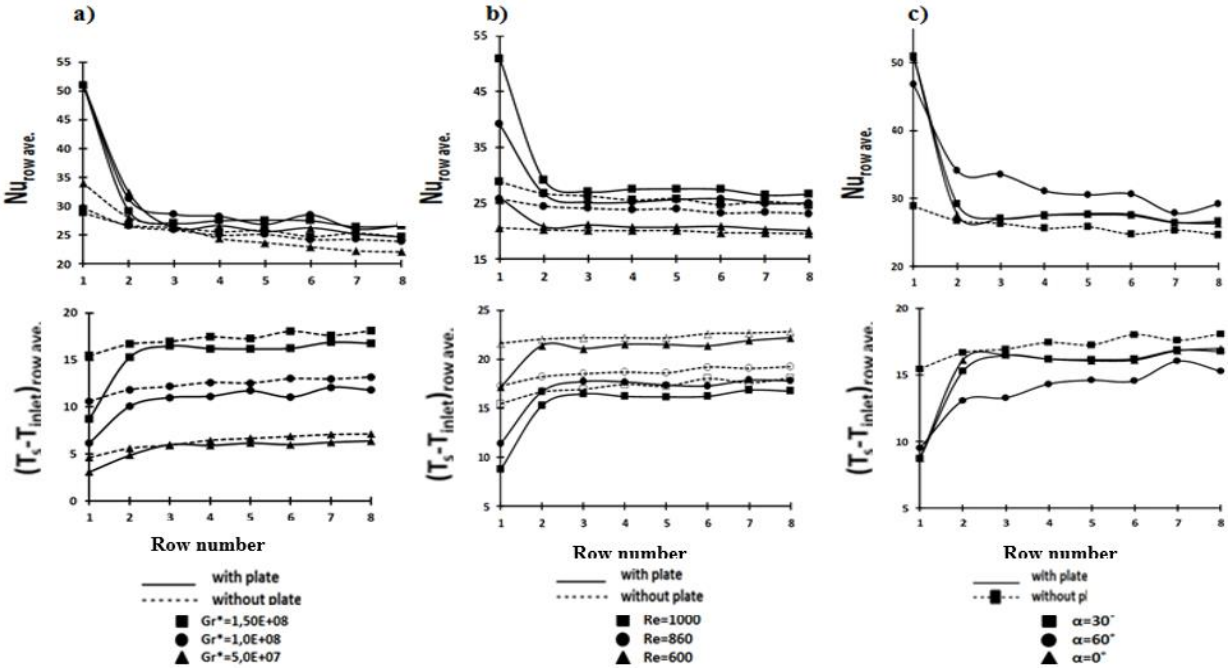

Figure 5. Variation of $Nu_{row\ ave.}$ ve $(T_s-T_{inlet})_{row\ ave.}$ for a) Gr* number, b) Re number, c) plate angle

In the case without plate for Gr * = 1.5x108, the velocity vectors direct towards the upper surface of the channel with the natural convection effect starting from the inlet of the heater zone, as understood from the y-z

plane velocity vectors, and this causes increase in the heater temperatures (Figures 7a and 7c). In the value of Gr*=5x107, mixed convection conditions occur. Therefore, the amount of air flow directed to the channel top surface due to the effect of natural convection decreases for the case with and without plate, and the temperature values in the heaters near the top surface decreases. (Figures 8 and 9).

Figures 10 and 11 show the velocity vectors and the temperature contours in the conditions with and without plate, respectively, as the Re number decreases to Re = 600. For the cases with and without plate, the Ri number increases to Ri = 19 and Ri = 20, respectively, and the heater temperaures incerases by increasing the amount of air directed to the top surface of the channel depending on the effect of natural convection. Another factor that causes the increase of temperature in the heaters near the top surface by using of plate, is increase in the amount of air directed to the center of the channel by hitting the surface of the heater with decreasing in the Re number.

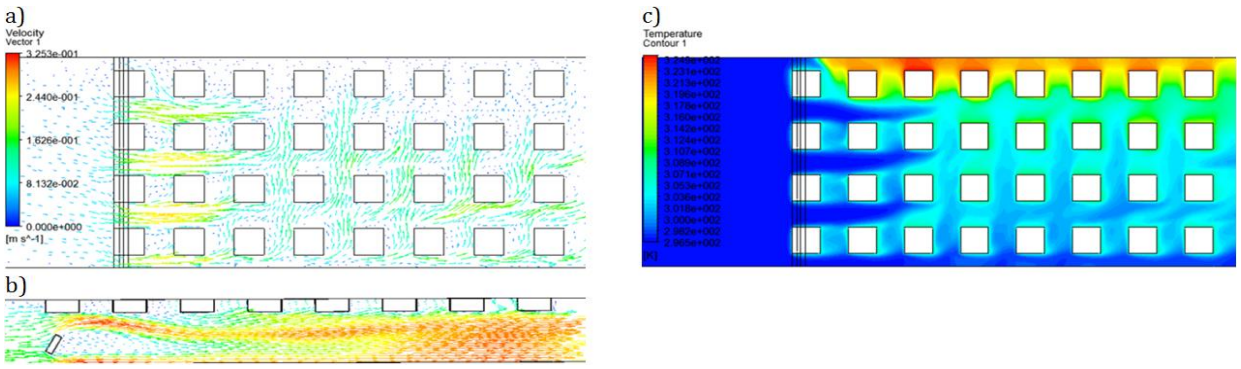

Figure 6. The case with plate a) y-z plane velocity vectors, x=25mm, b) x-z plane velocity vectors, y=75mm, c) y-z plane temperature contours, x=25mm (Gr*=1.5x10^8, Re=1000, α=30˚)

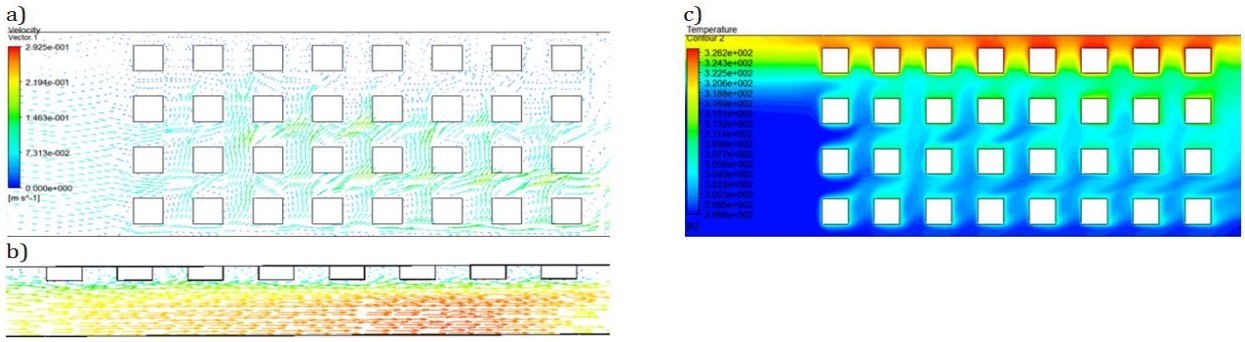

Figure 7. The case without plate a) y-z plane velocity vectors, x=25mm, b) x-z plane velocity vectors, y=75mm, c) y-z plane temperature contours, x=25mm (Gr*=1.5x10^8, Re=1000)

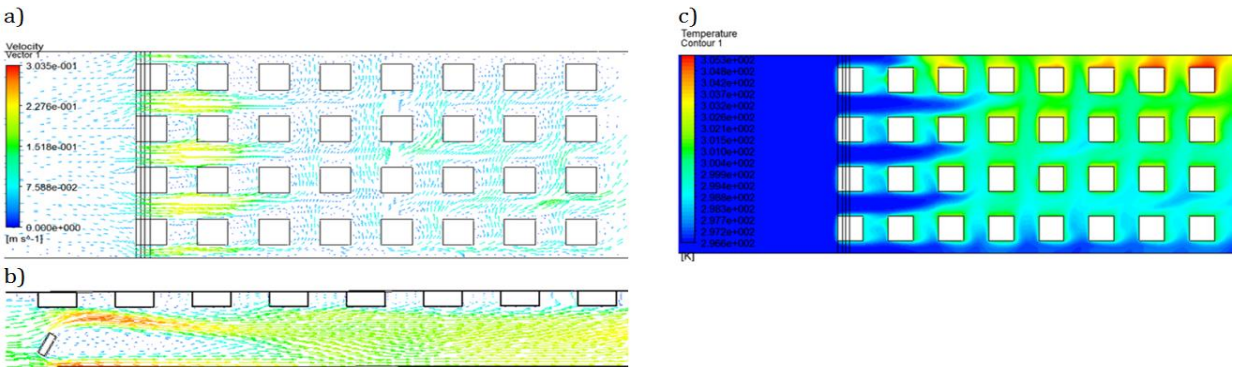

Figure 8. The case with plate a) y-z plane velocity vectors, x=25mm, b) x-z plane velocity vectors, y=75mm, c) y-z plane temperature contours, x=25mm (Gr*=5x10^7, Re=1000, α=30˚)

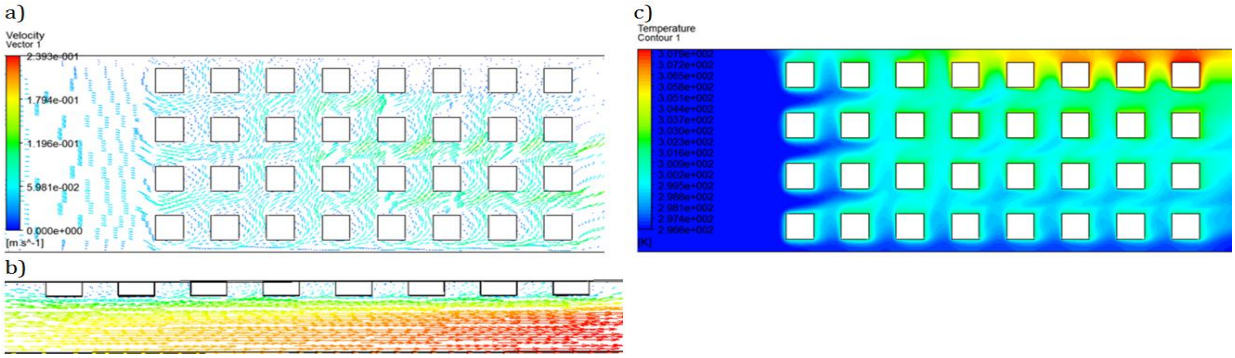

Figure 9. The case with plate a) y-z plane velocity vectors, x=25mm, b) x-z plane velocity vectors, y=75mm, c) y-z plane temperature contours, x=25mm ($Gr^*=5x10^7$, Re=1000)

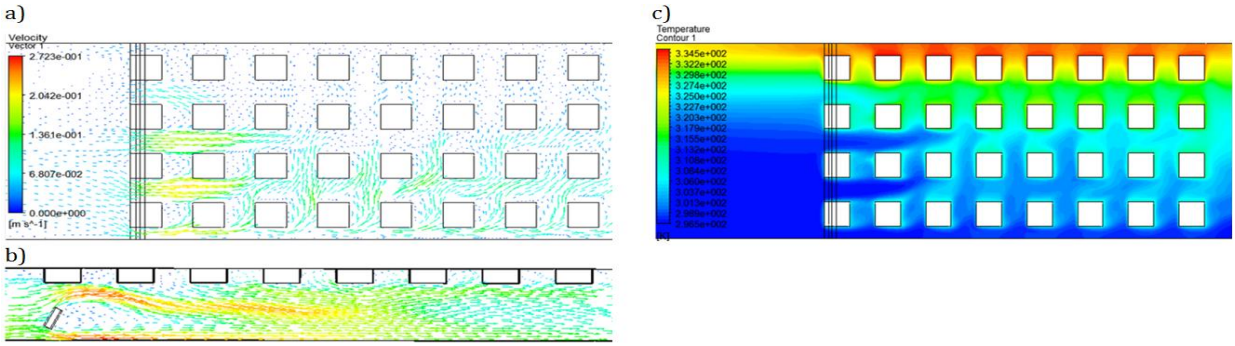

Figure 10. The case with plate a) y-z plane velocity vectors, x=25mm, b) x-z plane velocity vectors, y=75mm, c) y-z plane temperature contours, x=25mm ($Gr^*=1.5x10^8$, Re=600, α=30˚)

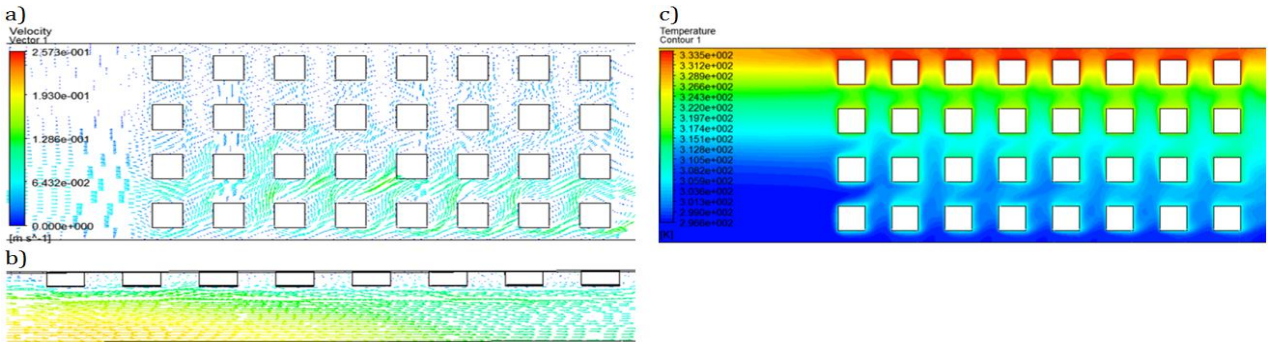

Figure 11. The case with plate a) y-z plane velocity vectors, x=25mm, b) x-z plane velocity vectors, y=75mm, c) y-z plane temperature contours, x=25mm ($Gr^*=1.5x10^8$, Re=600)

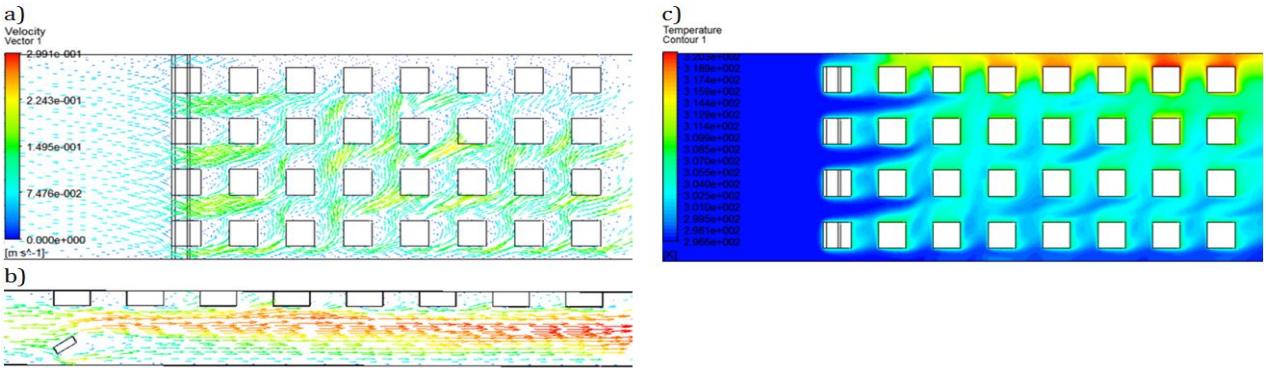

Figure 12. The case with plate a) y-z plane velocity vectors, x=25mm, b) x-z plane velocity vectors, y=75mm, c) y-z plane temperature contours, x=25mm ($Gr^*=1.5x10^8$, Re=1000, α=60˚)

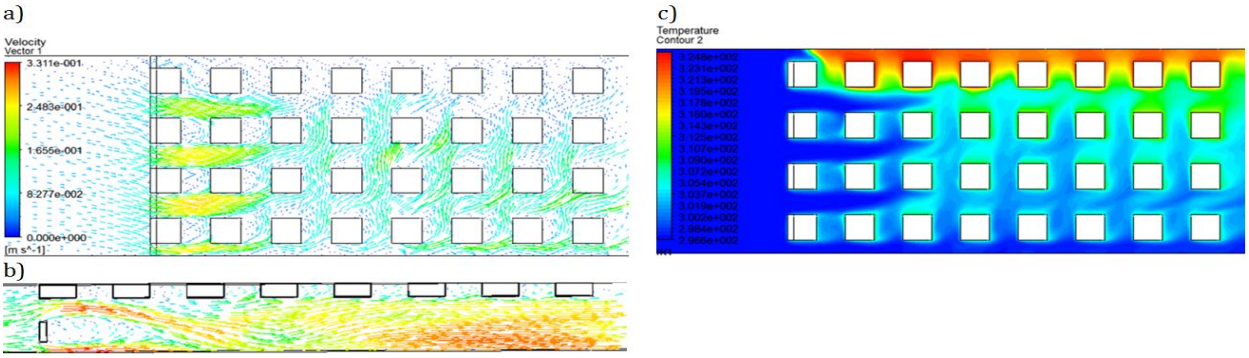

Figure 13. The case with plate a) y-z plane velocity vectors, x=25mm, b) x-z plane velocity vectors, y=75mm, c) y-z plane temperature contours, x=25mm (Gr*=1.5x108, Re=1000, α=0˚)

Figures 12 and 13 show velocity vectors and temperature contours for the plate angle of α = 60 ° and α = 0 °. When the x-z plane velocity vectors are examined for the case of α = 60 ° in which the highest heat transfer increase occurs according to the case without plate, it is understood that the air flow passing between the plate and the heater surface directs to the center of the channel by less amount than the other angle values. This provides the highest heat transfer enhancement for α = 60 °. For the plate angle α = 0 °, however, it is seen that the temperature values in the heater rows are approximately equal to the values in α = 30 °.

CONCLUSIONS

Results obtained from the numerical analysis, it is observed that the use of the flow routing plate increased the amount of heat transfer at different ratios and improves the cooling conditions for all of the parameter values with regard to the case without plate. The results obtained according to the parameters are summarized below.

As the heat flux values given to the heater surfaces increase, the Gr* number increases and the flow occurs under conditions in which natural convection conditions are predominant. This causes hot air to be squezeed between the heaters near the top surface for the condition without plate. The velocity of air at the inlet of the heater zone and the air movement between the heaters increase with the use of the plate. Thus, the use of plates provides further heat transfer enhancement in the conditions where the natural convection effect predominates.

The variation of the Re number is one of the most important factors affecting the flow regime. With the decrease in the number of Re, the effect of natural convection becomes dominant. The interpretation of the change for the Gr* number can also be made in relation to the Re number. The increase in the effect of natural convection makes the using of plate more effective than conditions without plate. However, when the natural convection effect rises above a certain level (Ri = 20, Re=600), the heater temperatures in the case with and without plate are close to each other. For this reason, the natural convection effect needs to be controlled.

The inclination angle of the flow routing plates changes the velocity of air at the inlet of the heater zone and the amount of air directed toward the center of the channel by hitting the heater surface. The increase in the amount of air directed to the center of the channel affects the cooling conditions for certain heater rows negatively. Therefore, when all heater rows are taken into consideration, it is seen that the highest heat transfer increase according to the case without plate is about %55 at the condition of α = 60˚.

NOMENCLATURE

A	heat transfer area, m^2
Ak	channel cross-sectional area, m^2
c_p	specific heat, kJ/kg.K
D_H	channel hydraulic diameter, m
g	gravitional acceleration, m/s^2
Gr	Grashof number, $Gr=(g\beta(T_s-T_{inlet})_{ave}.D_H^3)/v^2$
Gr*	modified Grashof number, $Gr^*=(g\beta q^{\cdot}_{conv.ave}.D_H^4)/kv^2$
h	convection heat transfer coefficent, $W/m^2.K$
H	channel height, m

k	thermal conductivty, W/m.K
L_P	plate width, m
$\dot{m}$	mass flow rate of air, kg/s
N_{fan}	theoretical fan power, W
$Nu_{row\ ave}$	row average Nusselt number, $Nu_{row\ ave.}= \dot{q}_{conv\ row\ ave} D_H/(k(T_s-T_{inlet})_{row\ ave.})$
P	air pressure, Pa
P_{atm}	atmospheric pressure, Pa
P_c	channel perimeter, m
$\dot{q}_{conv.}$	convection heat flux, W/m^2
Re	Reynolds number, $Re=(w_{inlet}D_H)/v$
Ri	Richardson number, $Ri=Gr/Re^2$
T	fluid temperature, K
T_{inlet}	air inlet temperature, K
T_s	heater surface temperature, K
u	x component of air velocity, m/s
v	y component of air velocity, m/s
w	z component of air velocity, m/s
w_{inlet}	air inlet velocity, m/s
W	channel width, m
ρ	air density, kg/m^3
α	plate angle
β	thermal expansion coefficent, 1/K
v	kinematic viscosity, m^2/s
μ	dynamic viscosity, kg/ms

REFERENCES

[1] Wu, H. W., & Perng, S. W. (1999). Effect of an oblique plate on the heat transfer enhancement of mixed convection over heated blocks in a horizontal channel. International Journal of Heat and Mass Transfer, 42(7), 1217–1235.
[2] Korichi, A., Oufer, L., & Polidori, G. (2009). Heat transfer enhancement in self-sustained oscillatory flow in a grooved channel with oblique plates. International Journal of Heat and Mass Transfer, 52(5–6), 1138–1148.
[3] Sohankar, A., & Davidson, L. (2001). Effect of inclined vortex generators on heat transfer enhancement in a three-dimensional channel. Numerical Heat Transfer; Part A: Applications, 39(5), 433–448.
[4] Sohankar, A. (2007). Heat transfer augmentation in a rectangular channel with a vee-shaped vortex generator. International Journal of Heat and Fluid Flow, 28(2), 306–317.
[5] Alahyari Beig, S., Mirzakhalili, E., & Kowsari, F. (2011). Investigation of optimal position of a vortex generator in a blocked channel for heat transfer enhancement of electronic chips. International Journal of Heat and Mass Transfer, 54(19–20), 4317–4324.
[6] Abdollahi, A., & Shams, M. (2015). Optimization of shape and angle of attack of winglet vortex generator in a rectangular channel for heat transfer enhancement. Applied Thermal Engineering, 81, 376–387.
[7]Caliskan, S. (2014). Experimental investigation of heat transfer in a channel with new winglet-type vortex generators. International Journal of Heat and Mass Transfer, 78, 604–614.
[8] Zhou, G., & Feng, Z. (2014). Experimental investigations of heat transfer enhancement by plane and curved winglet type vortex generators with punched holes. International Journal of Thermal Sciences, 78, 26–35.
[9] Chen, C., Teng, J. T., Cheng, C. H., Jin, S., Huang, S., Liu, C., Greif, R. (2014). A study on fluid flow and heat transfer in rectangular microchannels with various longitudinal vortex generators. International Journal of Heat and Mass Transfer, 69, 203–214.
[10] Xia, H. H., Tang, G. H., Shi, Y., & Tao, W. Q. (2014). Simulation of heat transfer enhancement by longitudinal vortex generators in dimple heat exchangers. Energy, 74(C), 27–36.
[11]Zdanski, P. S. B., Pauli, D., & Dauner, F. A. L. (2015). Effects of delta winglet vortex generators on flow of air over in-line tube bank: A new empirical correlation for heat transfer prediction. International Communications in Heat and Mass Transfer, 67, 89–96.
[12] Deshmukh, P. W., & Vedula, R. P. (2014). Heat transfer and friction factor characteristics of turbulent flow through a circular tube fitted with vortex generator inserts. International Journal of Heat and Mass Transfer, 79, 551–560.

[13] Li, H. Y., Chen, C. L., Chao, S. M., & Liang, G. F. (2013). Enhancing heat transfer in a plate-fin heat sink using delta winglet vortex generators. International Journal of Heat and Mass Transfer, 67, 666–677.
[14] Hatami, M., Ganji, D. D., & Gorji-Bandpy, M. (2015). Experimental investigations of diesel exhaust exergy recovery using delta winglet vortex generator heat exchanger. International Journal of Thermal Sciences, 93, 52–63.
[15] Gholami, A. A., Wahid, M. A., & Mohammed, H. A. (2014). Heat transfer enhancement and pressure drop for fin-and-tube compact heat exchangers with wavy rectangular winglet-type vortex generators. International Communications in Heat and Mass Transfer, 54, 132–140.
[16] ANSYS Fluent 14: User's Guide, ANSYS Inc: Canonsburg, November 2011.
[17] Kurşun B. Akış yönlendirici plakaların çıkıntılı ısı kaynaklarından karışık konveksiyonla laminer ısı transferine etkisinin deneysel ve sayısal olarak incelenmesi. PhD Thesis, Gazi University: Ankara, November 2015.
[18] Dogan, A., Sivrioglu, M., & Baskaya, S. (2006). Investigation of mixed convection heat transfer in a horizontal channel with discrete heat sources at the top and at the bottom. International Journal of Heat and Mass Transfer, 49(15–16), 2652–2662.